Modeling of Temperature Distributions in Mount Hope Bay Due to Thermal Discharges from the Brayton Point Station

Author(s): Craig Swanson, Hyun-Sook Kim, and Subbayya Sankaranarayanan
Source: Northeastern Naturalist, 13(sp4):145-172. 2006.
Published By: Eagle Hill Institute
DOI: http://dx.doi.org/10.1656/1092-6194(2006)13[145:MOTDIM]2.0.CO;2
URL: http://www.bioone.org/doi/full/10.1656/1092-6194%282006%2913%5B145%3AMOTDIM%5D2.0.CO%3B2

Modeling of Temperature Distributions in Mount Hope Bay Due to Thermal Discharges from the Brayton Point Station

Craig Swanson[1,*], Hyun-Sook Kim[1,2], and Subbayya Sankaranarayanan[1]

Abstract - Brayton Point Station is a 1600-MW electrical generating station located on Brayton Point, in Somerset, MA. The Station draws water from Mount Hope Bay at the Taunton and Lee Rivers for cooling purposes, and discharges the water back into the Bay, through a discharge canal. Mount Hope Bay is a shallow estuary located on the boundary between Rhode Island and Massachusetts. In connection with the renewal of the permit authorizing the withdrawal and discharge of cooling water, a series of studies on Mount Hope Bay were initiated by the owners of Brayton Point Station. These studies included both field and computer modeling components. A hydrothermal model capable of simulating the effects of Brayton Point Station on the Mount Hope Bay waters under a variety of operating scenarios was calibrated using the observed data. Additional cases were run to evaluate the effects of reduced discharges of heated effluent incorporating a cooling tower (enhanced multi mode operation) as well as the case of no discharge. Model results indicated that the temporal temperature variations occur over tidal to annual time scales. Seasonal variations were most discernible in the shallow upper reaches of the Bay, showing warmer than average temperatures during summer and cooler during winter. The calibrated hydrothermal model was also used to estimate the bottom area and water column volume coverage versus temperatures, which helps to quantify the effects of station heat load on the biological functions of winter flounder in Mount Hope Bay.

Introduction

Brayton Point Station

Brayton Point Station is a 1600-MW electrical generating station located in Somerset, MA, on Mount Hope Bay (MHB) at the confluence of the Taunton and Lee Rivers (Fig. 1). The Station's once-through cooling system draws subsurface water from MHB at two sites: from the Taunton River (eastern) side of Brayton Point for the coal-fired Units 1, 2, and 3, and from the Lee River (western) side for the oil-fired Unit 4. The water is pumped through the Station and then released via an open channel discharge, in this case a canal with a venturi structure at its mouth to enhance exit velocities into the Bay. The outfall characteristics generate a discharge jet, which enhances mixing and dissipates its momentum relatively close to the outfall. The subsequent thermal plume is advected with the tidal oscillations and wind-induced circulation in the area.

The Station discharges a maximum of 57 m^3s^{-1} (1300 mgd) of heated effluent when its four generating units are in operation. The Station currently

[1]Applied Science Associates, Inc., 70 Dean Knauss Drive, Narragansett, RI 02882. [2]Current address - School for Marine Science and Technology, 706 South Rodney French Boulevard , New Bedford, MA 02744. [*]Corresponding author - cswanson@appsci.com.

operates in accordance with a discharge permit allowing a 12.2 °C (22 °F) temperature rise between intake and outfall temperatures during regular operation and a 16.7 °C (30 °F) rise during piggyback operation. When the Station is operated in the piggyback mode, a portion of the heated water discharged from Units 1, 2, and 3 is diverted to the intake for Unit 4, eliminating water withdrawals from the Lee River. The upper temperature limit for effluent is 35 °C (95 °F).

Study area

The receiving water to which the Station effluent is discharged is MHB, a shallow estuary located on the state boundary between Rhode Island and Massachusetts (Fig. 1). It is the northeast component of the Narragansett Bay system, connecting to the East Passage through Bristol Ferry and to the Sakonnet River at Sakonnet (Fig. 2). Seventy percent of the Bay is less than 6 m deep at mean low water. A dredged channel 120 m (400 ft) wide and 10.5 m (34 ft) deep begins approximately 3 km (1.9 mi) northeast of the Mount Hope Bridge and continues up past Fall River into the Taunton River. A second channel, 10 m (33 ft) deep and 120 m (400 ft) wide, extends easterly and then northerly toward Fall River, and a third smaller channel,

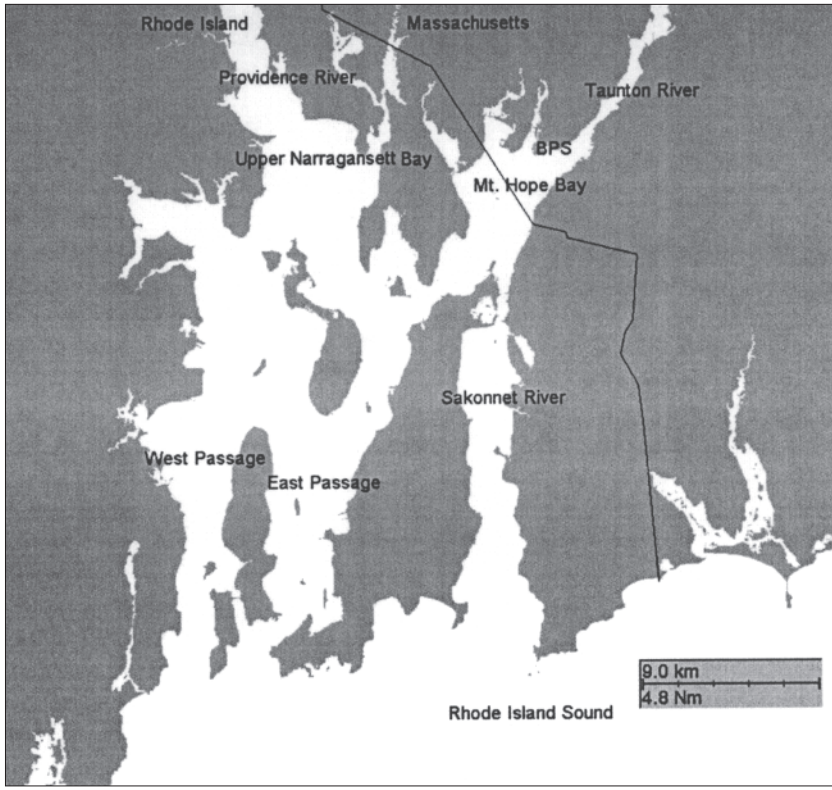

Figure 1. MHB study area shown in relation to Narragansett Bay.

10.4 m (34 ft) deep and 75 m (250 ft) wide, extends from the main channel in Fall River northwesterly to the Station. Three sub-embayments are located along the northern shore of the Bay to the west of the Taunton River mouth: the Lee, Cole, and Kickamuit Rivers.

Tidal fluctuations in the Bay range from 1.0 m (3.3 ft) at neap tide to 1.68 m (5.5 ft) at spring tide, with a mean range of 1.34 m (4.4 ft). Tidal currents are typically weak, 10–25 cm s^{-1} (0.3–0.8 ft s^{-1}) in the Bay, but can exceed 2 m s^{-1} (6 ft s^{-1}) in the narrows at Sakonnet. There is little amplitude or phase difference in tidal range throughout the Bay. The major freshwater source to the Bay is the Taunton River, with an annual average flow of 29.7 m^3 s^{-1} (1050 ft^3 s^{-1}), with flows dramatically falling to 9.4 m^3 s^{-1} (332 ft^3 s^{-1}) for the August mean and rising to 33.4 m^3 s^{-1} for the May mean (Ries 1990). The flow of the Taunton River influences the location and range of movement of the Station plume due to its proximity. The Cole River, the only other freshwater source, has a flow of 0.81 m^3 s^{-1} (28.7 ft^3 s^{-1}). The Lee and Kickamuit Rivers do not contribute measurable flows to the Bay.

Salinity-induced stratified conditions occur near the mouth of the Taunton River, and temperature-induced stratified conditions typically occur near the

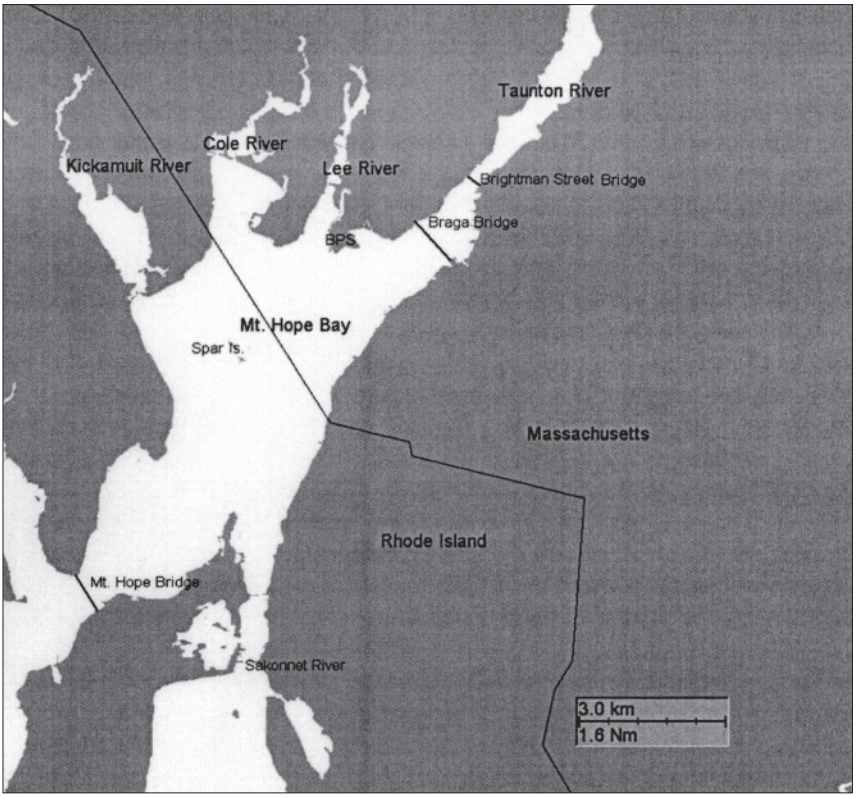

Figure 2. Location of Brayton Point Station on MHB.

Station outfall. These effects generally diminish as a function of distance from the Taunton River mouth and the Station outfall, respectively.

Hydrodynamic modeling studies in Mount Hope Bay

Huang and Spaulding (1995a) applied a three-dimensional numerical model (Huang and Spaulding 1995b) using rectangular grids to simulate transport processes in MHB due to combined sewer overflow (CSO) discharges. Model predictions of surface elevation, currents, salinity, and dye concentration showed good comparison with the observations, but they did not simulate the temperature distribution in MHB. Swanson et al. (1998) used a three-dimensional boundary-fitted hydrodynamic model to predict the temperature distribution in MHB. Skill assessment methodology used for calibrating and validating the predictions in Mount Hope Bay has been presented in Spaulding et al. (1999b). Results of model-data skill assessment (i.e., a formal statistical procedure to verify model performance) show that the model application was successful. Efforts are currently underway at SMAST (School for Marine Science and Technology, University of Massachusetts at Dartmouth) to construct an operational three-dimensional finite-volume-based hydrodynamic model (Chen et al. 2003) to also predict the thermal distribution in MHB.

Background of study

Starting in 1996, New England Power (NEP), then owner of the Brayton Point Station, initiated the application of a hydrodynamic model that could be used to simulate the effects of the Station's thermal discharge on MHB under different operating conditions. The purpose of this modeling was to support a comprehensive evaluation of the biological impacts of the Station's operation on MHB in connection with the renewal of the Station's National Pollutant Discharge Elimination System (NPDES) permit (USEPA-NE 2002). The effects of Station heat load on the biological functions of winter flounder in MHB is addressed in a companion paper by O'Neill et al. (2005), which uses an innovative biothermal model to link winter flounder biological processes to the hydrothermal model results. To develop this model, a two-component study was performed:

1. Physical measurements of the Bay were collected to determine the spatial and temporal distribution of circulation and water temperature during different seasons.
2. A simulation model was constructed to predict the hydrodynamics and thermal structure of the Bay under different Station thermal loads and environmental conditions. The model was calibrated and verified with the data collected during the field program.

The calibrated model is then used to estimate the bottom area and water-column volume coverage versus temperatures in order to support bio-thermal modeling.

Hydrothermal Field Data Collection in Mount Hope Bay

An extensive program of hydrographic and thermal mapping observations in MHB was undertaken to calibrate and validate the hydrothermal model developed in this study. Table 1 gives a summary of field programs supporting hydrothermal modeling of MHB, including month-long moored hydrographic deployments that measured temperature, salinity, velocities, and tidal elevation under summer, fall, and winter conditions, and thermal-mapping studies conducted for two- to six-week periods during different seasons to obtain horizontal and vertical temperature data. A brief description of the hydrographic and thermal-mapping surveys is given in the following sections.

Month-long hydrographic surveys

Month-long studies were conducted during the late summer in 1996 and 1997 using several moored instruments, including multi-parameter monitors measuring temperature and salinity, current meters, and a water-level sensor. Figure 3 shows locations of long-term monitoring stations for the August 1997 study. The observations from these stations were used for calibrating the model. Also, part of this study was acquisition of related data collected by various organizations, including light intensity, wind speed and direction, air temperature, river flow, and Brayton Point Station cooling-water flow and temperature. Results from these long-term surveys are documented in ASA (1996) for the 1996 survey and Rines and Schuttenberg (1998) for the 1997 survey.

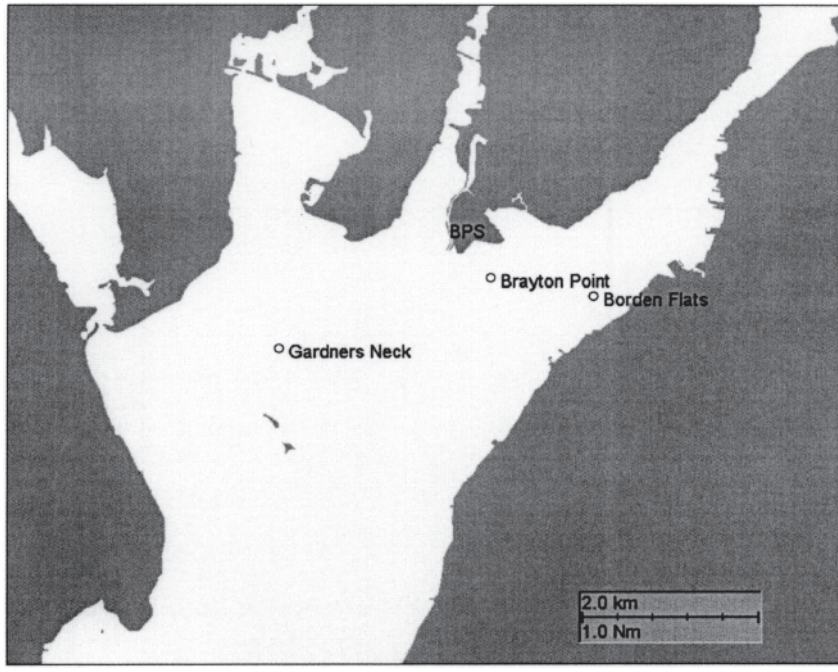

Figure 3. Location of long term monitoring station for August 1997.

Table 1. Summary of field programs supporting hydrothermal modeling of Mount Hope Bay.

Program	Period covered	Time of year	Measurements	Number of stations
Routine monitoring (MRI)	1972 to present	Full year	Temperature, salinity, and DO profiles	6–7
Long-term hydrographic survey	1996	August	Full month of surface and bottom temperature, salinity, DO, and velocity	2
Long-term hydrographic survey	1997	August	Full month of surface and bottom temperature, salinity, DO, and velocity	4
Short-term hydrographic survey	1996 (twice)	August	Temperature, salinity, and DO profiles at four consecutive slack tides	17
Short-term hydrographic survey	1997	August	Temperature, salinity, and DO profiles at four consecutive slack tides	17
Thermal mapping	1997	May–June	5-min. measurements of temperature at five depths per station	30
Thermal mapping	1997	August–September	5-min. measurements of temperature at five depths per station	30
Thermal mapping	1998	September	5-min. measurements of temperature at five depths per station	30
Short-term hydrographic survey	1998	September	Temperature, salinity, and DO profiles four times over tidal cycle	21
Thermal mapping	1999	February–March	5-min. measurements of temperature at five depths per station	31

Currents are important in MHB because they move the thermal plume in response to tides, river flow, and winds. A double pulse characterizes the flood tide in Mount Hope Bay. Kim and Swanson (2001) showed that the interactions among M_2, M_4, and M_6 tides result in double-peaked flood profiles that typify currents in MHB. The double peaks that occur during flood tide in Mount Hope Bay are clearly seen in a typical time series of observed mid-depth current speeds at Fall River in Figure 4. The first pulse is typically somewhat smaller than the second, although it varies in magnitude from almost nonexistent to equal in magnitude to the second. In general, the mean current speeds were 13.5 cm s^{-1} at the Borden Flats Station, 10.5 cm s^{-1} at Brayton Point Station, and 5.5 cm s^{-1} at the Gardners Neck Station. The mean speeds affecting the Station thermal plume were in the range from 5 to 10 cm s^{-1}, a relatively low velocity.

The tidal effect on salinity variation was quite evident at the Borden Flats Station, where diurnal variations as large as two parts per thousand were seen at the surface and more than one part per thousand at the bottom. At Gardners Neck, there was hardly any evidence of a tidal signal in the salinity record near the surface and evidence of only a small signal at the deep sensor. The records at Brayton Point Station were intermediate between these two. There was a strong tidal variation (at 12.42 hours) evident in the temperature record at the surface at the Borden Flats location, but this was sometimes overwhelmed by a diurnal

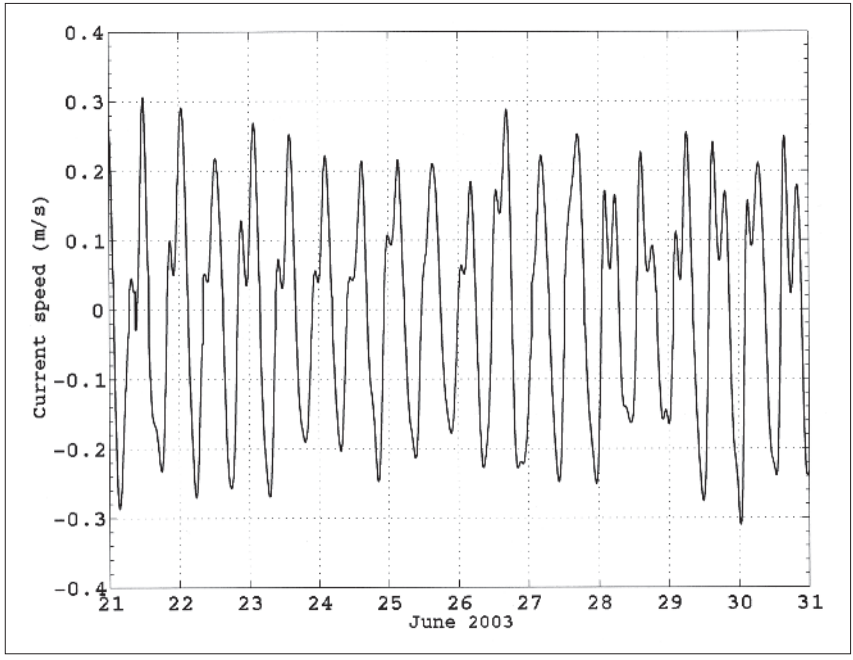

Figure 4. Observed mid-depth acoustic Doppler profiler currents at Fall River, obtained from the National Ocean Service.

signal (24 hours). A tidal signal was only occasionally evident at the bottom at this station. At the Gardners Neck location, the diurnal variation was generally greatest, although this varied through the month. At the near-bottom sensors, the short-term temperature changes were very irregular. By comparison, there was a strong tidal element to the temperature record at all three depths at the Brayton Point location, with the largest swing often occurring at the surface, where a diurnal component was added to the temperature changes.

Thermal mapping surveys

An extensive field program to map the thermal structure in space and time in MHB was conducted. Four major surveys were conducted: May 19–June 4, 1997, August 8–September 12, 1997, September 1–18, 1998, and February 12–March 22, 1999. Figure 5 shows the locations of the thermistor strings for the May 1997 survey. The strings were generally laid out in arcs of concentric circles centered on the Station outfall, with radii of 0.5, 1, 2, and 4 km. These thermistor strings consisted of buoyed lines with self-logging thermistors attached at 0.25-, 0.5-, 1-, 2-, and 4-m depths. Results from these thermistor surveys, including animations on CD, are documented in Rines (1998) for the

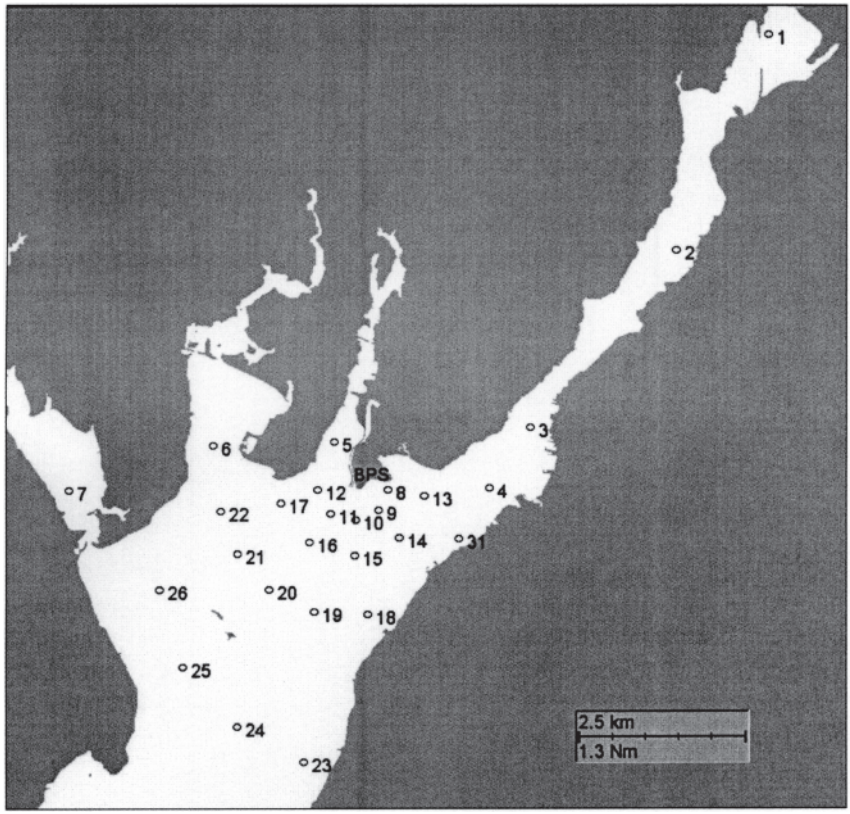

Figure 5. Location of thermistor strings for May 1997 field study.

1997 surveys, Rines (1999) for the 1998 survey, and Swanson et al. (1999) for the 1999 survey. A description of these surveys is also found in Appendix E of USGenNE (2001).

The thermistor surveys show that, in the Taunton River, events were driven mostly by tides, weather, and river flows, with no effect from the Brayton Point Station plume. In MHB, the temperature pattern was distinctly tidal in nature, with the most regular cycles seen at the deepest thermistor, where weather influences were mitigated. The shallowest thermistor recorded the largest temperature peaks, probably due to the effects of daily warming and cooling at the air/water interface. Close to the outfall, strong temperature peaks with tidal periodicity were common. No significant vertical stratification was seen in the observations. At middepths during winter, these temperatures peaked, representing the passing Brayton Point Station plume. This can exhibit a stable condition, since the surface discharge consisted of warm, more saline water into a receiving water that was colder and fresher. It is to be noted that the intake is located at the bottom (hence draws more saline water), while the discharge is located at the surface. During summer, the plume was consistently at the surface. There was no upwelling or downwelling event to be addressed, since the vertical profiles of the month-long moorings did not display any bending thermoclines.

A series of aircraft overflights using sensors to measure radiance were conducted concurrently with the thermistor in-situ surveys. Processing of the overflight data and analysis of the results are described in Fisher and Mustard (2004).

.

Simulation Model

Description of the WQMAP model system

WQMAP (Water Quality Modeling and Analysis Program), a modeling system developed by ASA and the University of Rhode Island, is an integrated system for modeling the circulation and water quality of estuarine and coastal waters (Spaulding et al. 1999a). The system has a suite of integrated environmental models, including a boundary-conforming grid-generation model, a three-dimensional hydrodynamic model, and a set of pollutant transport and fate models (single- and multiple-constituent and WASP5 [Water Quality Analysis Simulation Program]). All operate on a boundary-conforming grid system and are supported by an embedded geographic information system and environmental data management tools. WQMAP is configured for operation on a personal computer running a Windows operating system. Color graphics and animations are used to display model predictions. The system is structured to facilitate application to any geographic area.

WQMAP's hydrodynamic model solves the three-dimensional conservation of water mass, momentum, salt, and energy equations on a spherical, non-orthogonal, boundary-conforming grid system. The boundary-fitted model matches the model coordinates with the shoreline boundaries of the

water body, accurately representing the variable geometry of the coastal features of MHB. A sigma stretching system is used to map the free surface and bottom to resolve bathymetric variations and the vertical structure. Development of the boundary-fitted model approach has proceeded for almost two decades (Spaulding 1984; Swanson et al. 1989; Muin and Spaulding 1996; Muin and Spaulding 1997a,b). A detailed description of the governing equations, numerical solution methodology, and in-depth testing against analytic solutions for two- and three-dimensional flow problems can be found in the papers cited above. WQMAP has been applied to many different types of coastal problems, including thermal plume simulations in Sandwich, Weymouth, and Saugus, MA; Vernon, VT; and Jubail, Saudi Arabia.

The WQMAP hydrodynamic (or hydrothermal) model can simulate the effects of tide, river flow, air temperature, solar radiation, and wind-induced environmental forcing. The observed meteorological and thermodynamic data at Rhode Island's T.F. Green Airport (located 19 km southwest of Brayton Point Station) was obtained from the Northeast Regional Climate Center (NRCC) at Cornell University. The environmental heat transfer submodel at the water surface, which closely follows Edinger et al. (1974), contains an explicit balance of shortwave solar radiation, longwave atmospheric radiation, longwave radiation emitted from the water surface, convective (sensible) heat transfer, and evaporative (latent) heat transfer between water and air. More details on the heat transfer model are reported in Appendix B of Swanson et al. (1998).

Model application

The first step in the setup of a hydrodynamic model is generating a grid that defines the study area of interest. For the current study, the northern portion of MHB is the focus. Experience with previous model applications suggests, however, that open boundaries should ideally be placed away from the area of interest to minimize their effect on the interior solution. The grid used for this application is shown in Figure 6. Here, the full grid encompasses the northern half of Narragansett Bay and the Sakonnet River and extends to the head of tide in the Taunton River. There are a total of 3300 water grid cells covering the area. The grid in Narragansett Bay and the Sakonnet River is purposely coarse (1 km [0.6 mi]) to minimize the calculations required yet still provide reasonable predictions. Typical grid cell dimensions in the southern portion of the Bay are 200 to 300 m (650 to 1000 ft). The grid is finer in the area near the Station (Fig. 7) to better resolve the circulation affecting the thermal plume. Here, the typical grid cell dimensions are 50 to 100 m (160 to 330 ft). A depth value must be assigned to each grid cell. A database of bathymetric soundings (NGDC 1996) with associated latitude and longitude for the area was accessed, and depths were interpolated onto the grid. The depths in the grid were manually edited with the depths from the NOAA charts, to represent the channels. The 120-m-wide channels are adequately resolved using two cells.

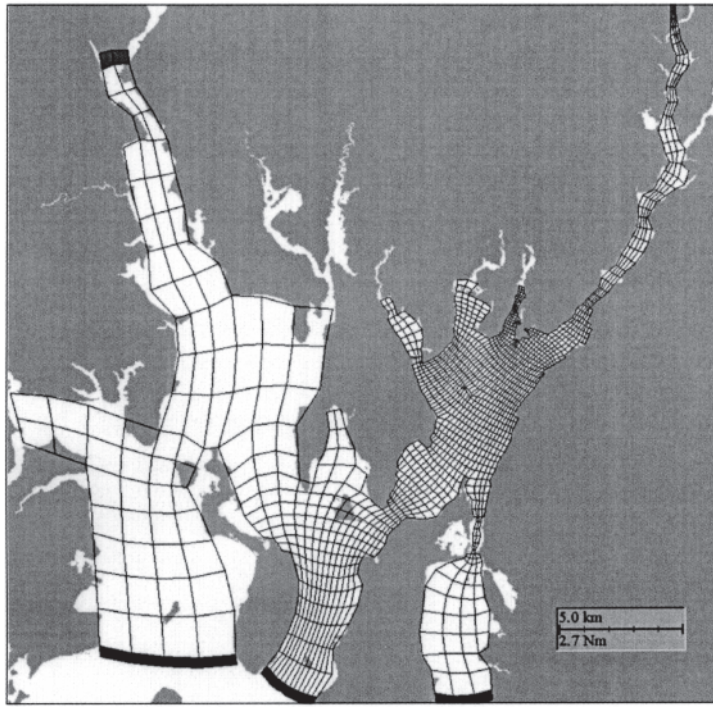

Figure 6. Full model grid of greater Mount Hope Bay.

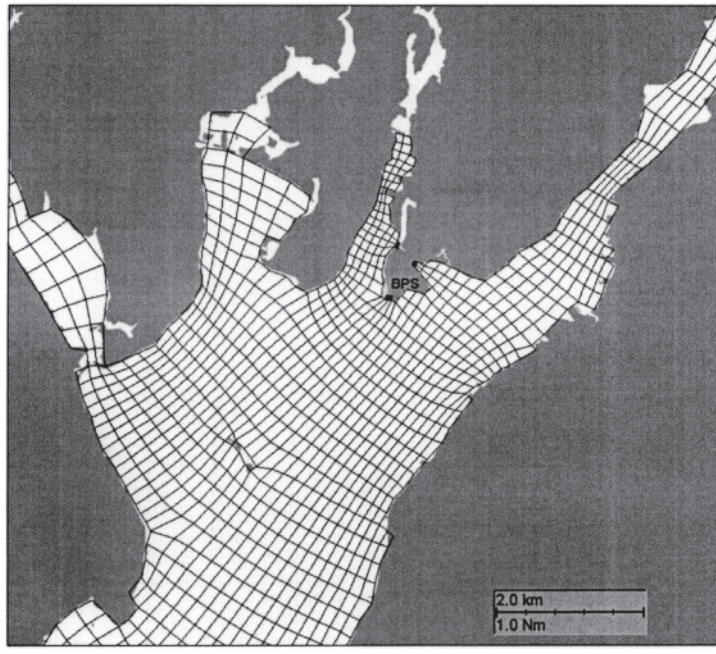

Figure 7. Model grid of area around the Brayton Point Station.

Forcing functions are used in the model to drive the circulation of water throughout the Bay, which in turn affects the location of the thermal plume and the Bay-wide temperature structure. The forcing functions are applied at the model open boundaries. For the Brayton Point Station application, the open boundaries are located in Narragansett Bay, in the Sakonnet River, at the head of the Taunton River, at the air-sea interface, and at the Station's intake and discharge. These time-varying functions were flows (river flow), atmospheric effects (winds, temperature, solar radiation), water level (tidal and non-tidal), density gradients (salinity held constant at 32 psu and time-varying temperature), and Station loads (flow rate and temperature increase). The water-level open-boundary condition allowed simulations of both periodic and non-periodic events. The outfall discharge did not exhibit any periodicity; instead, it was steady with flows remaining constant for days. The wind speed and direction were converted to wind stress using a standard wind-stress formulation given in Muin and Spaulding (1996).

Model calibration

Calibration and confirmation (verification) are important steps in the process of applying a model to a specific problem, particularly for those models that contain many degrees of freedom. The calibration/confirmation process is a structured approach to evaluate how well a model can reproduce observations. The calibration procedure (McCutcheon et al. 1990) followed for the Brayton Point Station application included these steps:

1. Reproduce elevation and velocities at selected locations by adjusting bottom-friction and eddy-viscosity coefficients.
2. Reproduce distributions of natural tracers (salinity) by adjusting eddy diffusivities.
3. Reproduce temperature distributions by adjusting flux rates to the atmosphere. Since the meteorological observations were from the land-based station at Green Airport, air temperatures used for the surface heat-flux model were adjusted slightly so that the error between the observed and model-predicted temperatures was minimized. This adjustment in air temperature was supported by a limited set of observed air temperatures in the Bay. In addition, the Station thermal load was distributed over grid cells adjacent to the discharge.

Confirmation or verification of the model is performed with an independent set of data to determine how well the model can predict the distribution of the model variables. It is expected that the verification results will be similar to the calibration results. If not, then a review is warranted to determine what model parameters were responsible. If necessary, the model is recalibrated through a process of optimization.

A series of comparisons are used to provide measures for the success of the calibration and confirmation steps. These measures are both qualitative and quantitative. The qualitative comparison of model results and observations depends on data dimensionality. For example, a time series of data

collected at a particular site can be plotted together with model output to provide a visual comparison. This comparison can provide information on the suitability of the model to simulate the range of variability evident in the observations. The most direct way to provide a qualitative comparison is to plot the model predictions and the observed data for each variable over the time of the simulation. The error in model-predicted surface elevations and currents met the target criteria given in McCutcheon et al. (1990), and the details are given in Spaulding et al. (1999b). Quantitative estimates of the error between the observed and model-predicted temperatures were obtained in this study to get an idea about the predictive capability of the model. The primary focus of the calibration process is to

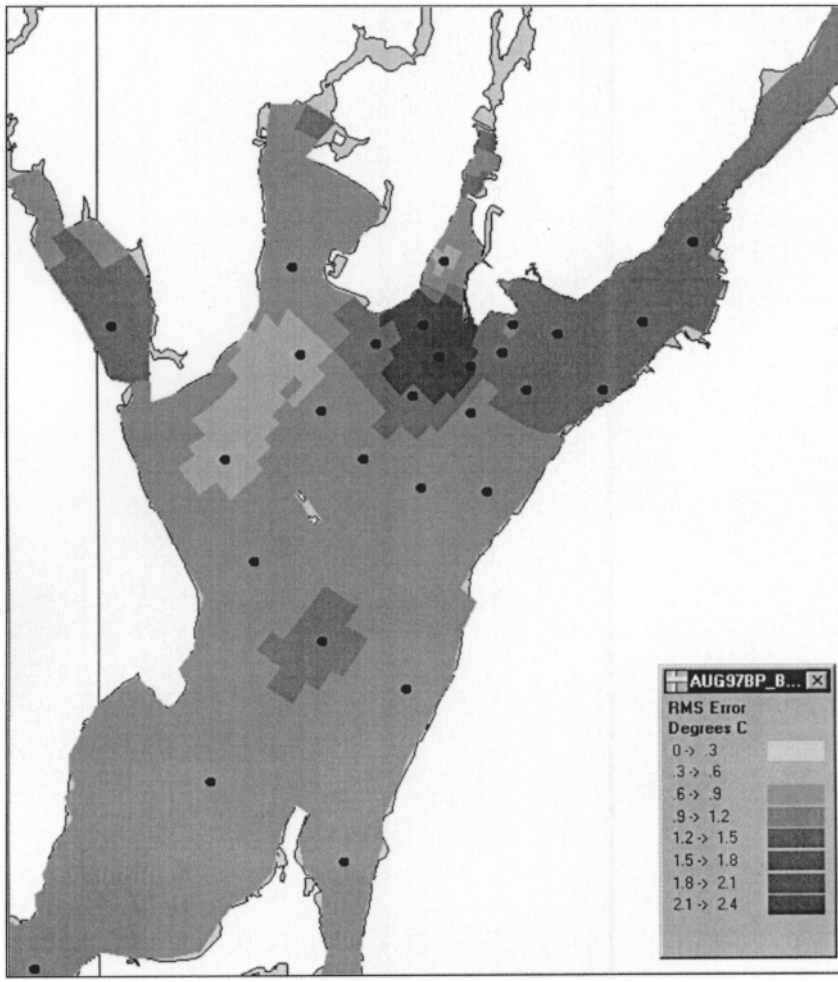

Figure 8. Spatial distribution of root mean square (RMS) errors between the observed and predicted temperatures at a depth 0.25 m from the surface for the August 97 period. (Error range increment in the color contour legend is 0.3 °C.)

adjust appropriate model parameters to optimize the comparison to a data set of observations. The parameters, as discussed in the previous sections, include bottom friction, horizontal and vertical dispersion, and atmospheric exchange rates. The August 1997 data set was chosen for calibration in collaboration with the Technical Advisory Committee (TAC) because it was more extensive and complete than the 1996 data set. This was due, in part, to a better understanding of the circulation in MHB gained from analysis of the 1996 data. The period of comparison was from August 1 through September 2, 1997. Figure 8 shows the contours of root mean square (RMS) error between the observed and model-predicted surface (0.25 m from the surface) temperatures in MHB, with errors less than

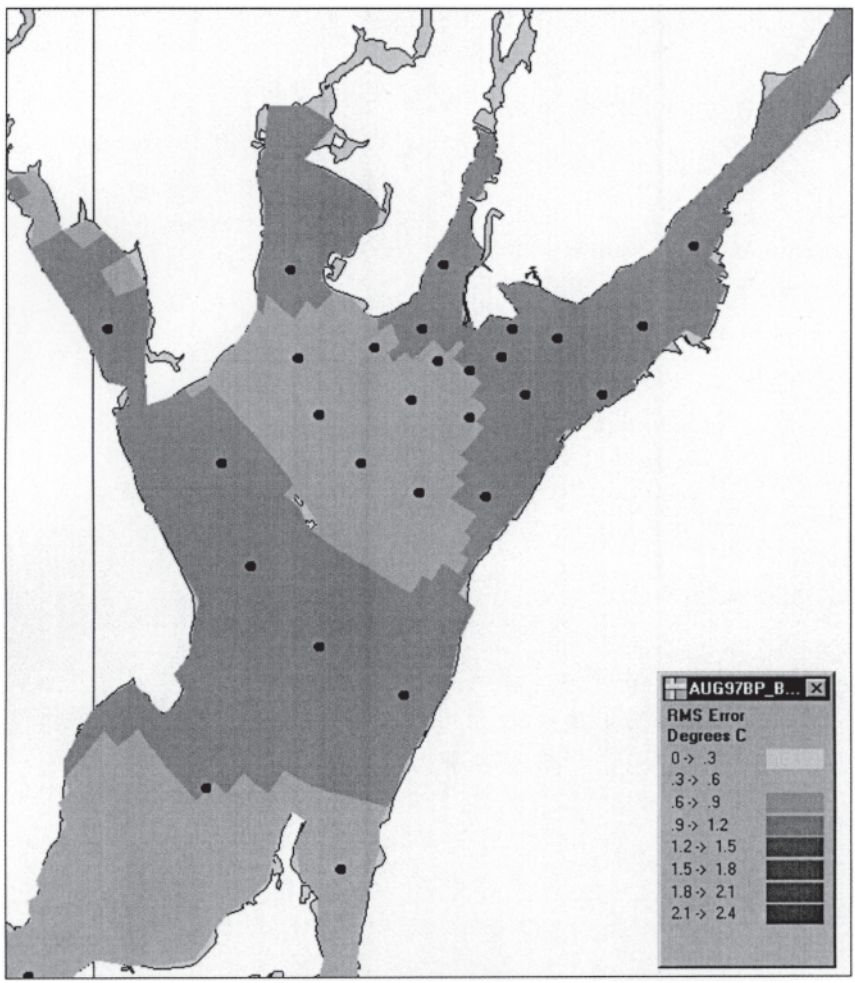

Figure 9. Spatial distribution of root mean square (RMS) errors between the observation and predicted temperatures at a depth 4.0 m from the surface for the August 97 period. (Error range increment in the color contour legend is 0.3 °C.)

1.5 °C. Figure 9 shows the spatial distribution of RMS error between the observed and predicted temperatures at a depth 4 m from the surface, with errors less than 1 °C.

Model verification

The purpose of the verification (confirmation) process is to determine how well the model performs in comparison to a data set that is independent from that used in the calibration step. All of the parameter values used in the calibration are held constant for the verification. The August 1996 data set was initially chosen for confirmation (verification) because it was less extensive and complete than the 1997 data set. This is described in detail in Swanson et al. (1998). Ultimately, the TAC requested that a different season be used for model verification, so the winter 1999 was used. Figure 10 compares the observed and predicted temperatures at the surface for a series of thermistors in the winter of 1999. A similar comparison of the observed and predicted temperatures at a depth 4 m from the surface is shown in Figure 11. The model successfully simulates the multiple time scales (tidal, daily, and weekly) seen in data during this period. Additional information on the model–data comparison can be found in the winter verification report (Swanson et al. 1999).

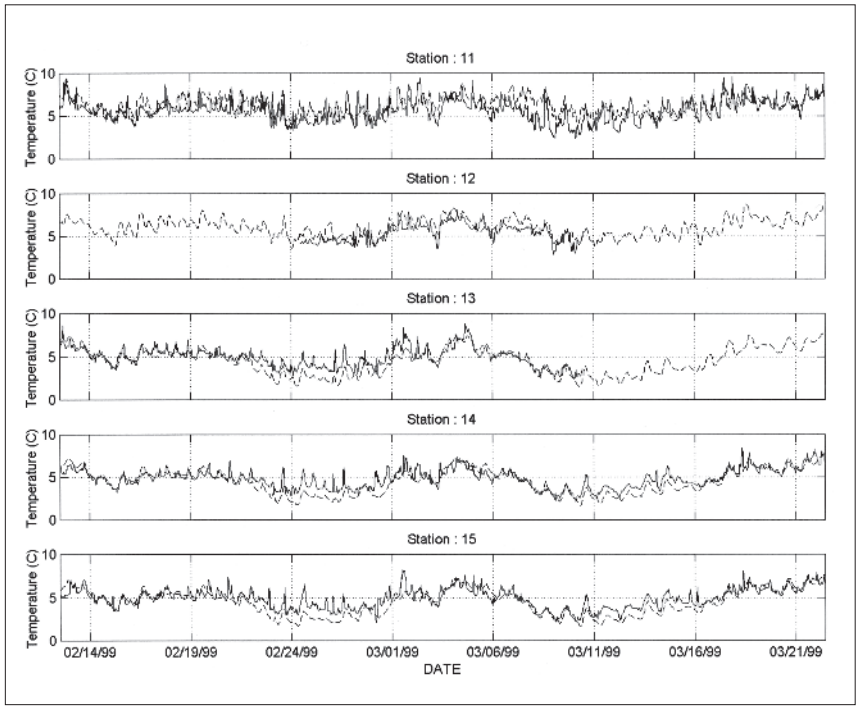

Figure 10. Temperature comparison between observations and model predictions at 0.25 m from surface at five sites during winter of 1999. (The solid lines denote observations and the broken lines denote model predictions.)

Model optimization

Optimization of the hydrodynamic model of MHB was performed in response to a request from the TAC to refine the model to simulate, as closely as possible, observed temperature conditions in the Bay. The specific focus of the optimization was to match the observed temperatures acquired during the thermistor surveys of summer 1997, winter 1999, and spring 1997 with an emphasis on thermistors 18, 19, 20, 21, and 22 (Fig. 5) with their locations forming a ring (Ring 3, located at 2 km radius from the Station outfall) that is generally coincident with the Massachusetts/Rhode Island boundary. As a result of the optimization, the vertical and horizontal temperature dispersion rates, local atmospheric temperature, and Station thermal load were slightly modified.

The measures that were used in the quantitative model assessment were the mean difference (MD) between model prediction and observed data and the RMS error between the two. These statistics were generated for individual meter locations as well as aggregations of meters (thermistors by depth, thermistors by section of the Bay, thermistors by radial distance from the Station, etc.). In Table 2, a summary of the statistical comparisons to the thermistors shows the success of the optimization to the set of thermistors on Ring 3, particularly for the MD.

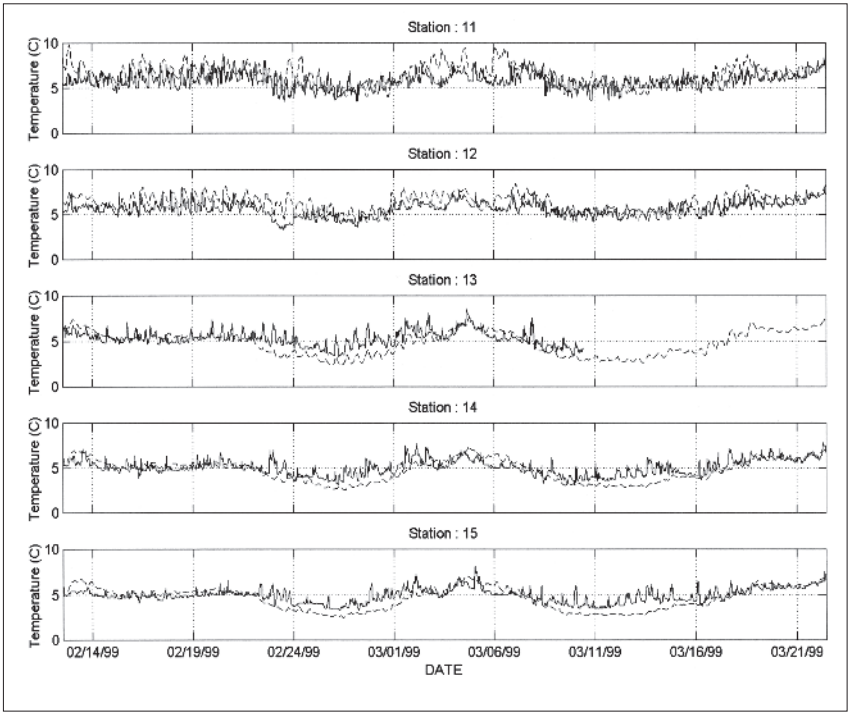

Figure 11. Temperature comparison between observations and model predictions at 4.0 m from surface at five sites during winter of 1999. Solid lines denote observations and the broken lines denote model predictions.

Two memoranda were prepared in July 2000 to document this analysis. They are found in Swanson et al. (2001). Ultimately, the TAC accepted the WQMAP model in September 2000 as suitably calibrated for use in predicting the thermal structure of MHB under both different seasonal conditions and Station loading conditions.

Selection of model runs

The final step in the modeling process was the selection of the operating scenarios to be evaluated. The year 1999 was determined to be a reasonable worst-case warm-water year and was therefore selected to provide the environmental conditions under which the cases were run. Although many scenarios were run and presented during the course of the studies in support of the Brayton Point Station's permit application, this discussion focuses on three that span the range from existing operations (known as MOAII), an enhanced multimode (EMM) operating scenario that significantly reduced thermal discharge, and the no-plant case. A summary of the model runs is shown in Table 3. Mean Station flow, temperature increase, and heat load are shown for comparison.

Results

Plume characterization

Figures 12 and 13 show typical spatial distributions of temperatures in MHB at maximum ebb and maximum flood, respectively, for the EMM hydrothermal model run. The inserts on the figures show the sectional view of the plume from the outfall. At maximum ebb, the thermal plume extends in the south-southwest direction (Fig. 12), since the ebb current moves in that direction. As the tide turns, the plume generated during the

Table 2. Comparison of model-predicted and observed temperature data. MD = mean difference; RMSE = root mean square error.

	MD (°C)	RMSE (°C)
Summer 1997		
All thermistors	-0.21	0.83
Ring 3	0.03	0.57
Winter 1999		
All thermistors	-0.67	1.13
Ring 3	-0.10	0.71
Spring 1997		
All thermistors	0.69	1.12
Ring 3	1.03	1.34

Table 3. Summary of hydrothermal model runs for the warm year 1999.

Operating scenario	Flow (mgd)	Temperature increase (°F)	Heat load (tBTU/mo)	Description
MOA II	868.15	14.71	3.18	Actual operation data for 1999
EMM	593.38	14.64	2.25	Enhanced multimode
No-plant	0.00	0.00	0.00	No Station operation

previous ebb is moved north, while the plume generated during the flood moves towards the mouth of the Taunton River. At maximum flood (Fig. 13), the remnants of the ebb plume are seen to the west of the Station discharge, while the just discharged flood plume is seen to the east.

The WQMAP hydrothermal model output was processed to generate a series of products needed for the biological assessment:

1. Daily averaged total temperatures for water-column volume and bottom area,
2. Daily averaged temperature increases over background (no-plant) conditions,
3. Distributions of Bay volume and bottom area for a range of total temperatures, and
4. Distributions of Bay volume and bottom area for a range of temperature increases over background conditions.

These products were generated for the historical and hypothetical Station loads listed in Table 3 using 1999 environmental conditions.

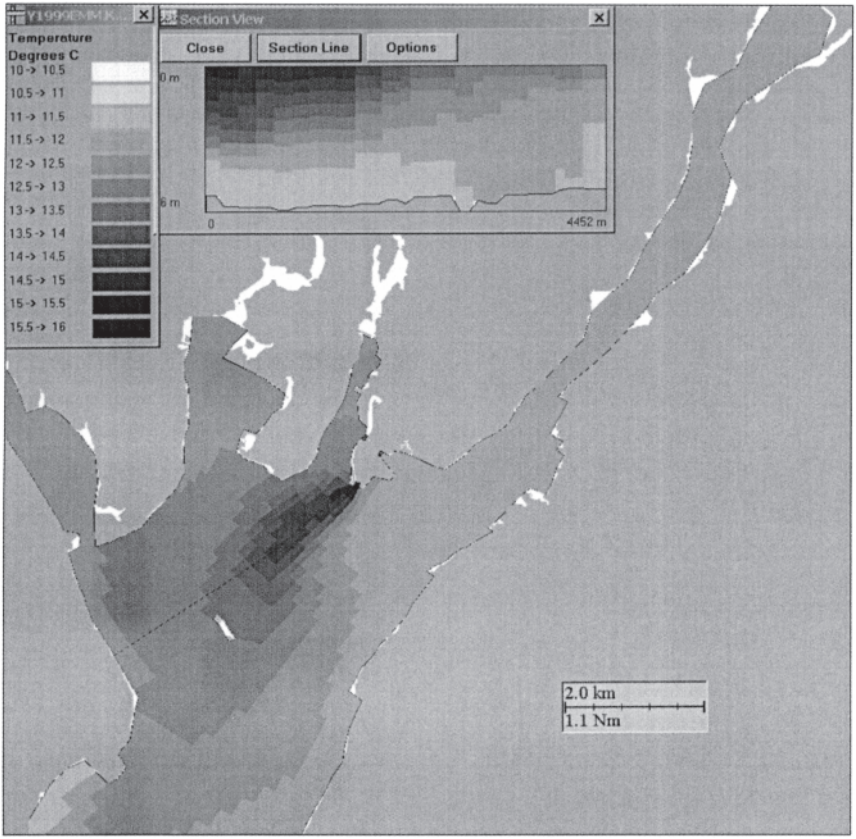

Figure 12. Plan view of distribution of surface temperatures in MHB for EMM model run at maximum ebb. Vertical cross-sectional view of the plume from the outfall is shown in the insert.

A comparison of typical results from the different Station loads is shown in Figures 14 to 19. Each figure shows a plan view of the daily averaged temperature distribution for one representative day during the winter and summer periods of biological significance. Figures 14 and 15 show the results for MOA II, which has the highest load. The upper panel (Fig. 14) shows the water-column volume winter plume offset to the southwest due to environmental conditions (higher river flow) compared to the lower panel (Fig. 15) for summer conditions. Peak temperatures occur in the immediate area of the discharge, with the plume oriented toward the southwest away from the discharge. The results are similar but reduced in magnitude for the bottom area during both summer and winter. The EMM scenario, shown in Figures 16 and 17, generates smaller plumes with lower peak temperatures than MOA II because its heat load is lower. Figures 18 and 19 show the same results for the environmental background (no-plant) scenario. There are small variations over the Bay (less than 1 °C) during the different seasons, with the northern portions slightly colder in winter and warmer in summer.

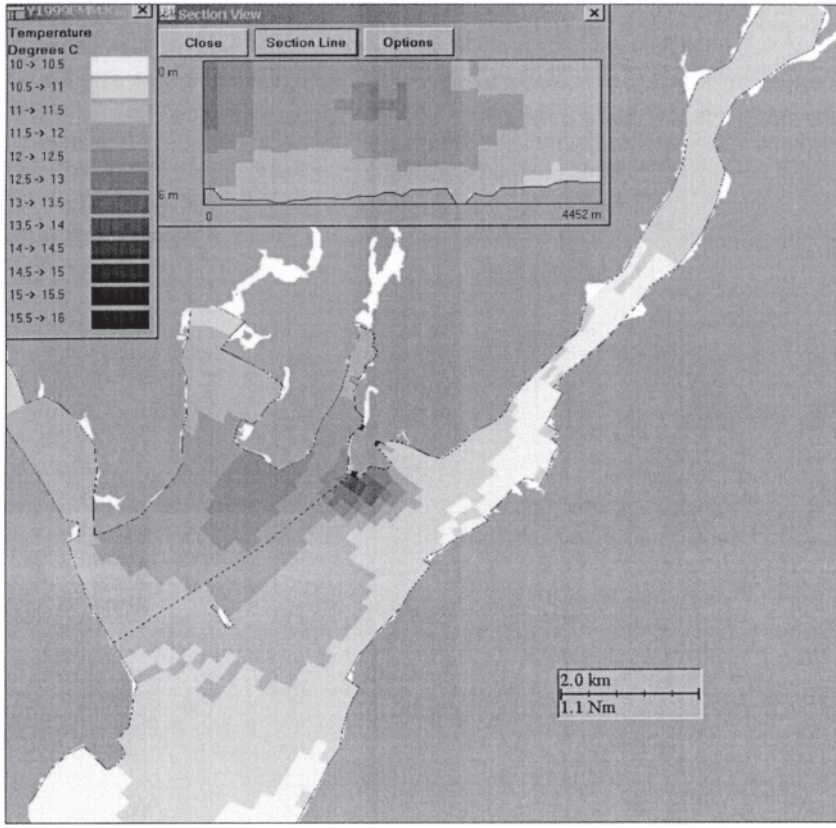

Figure 13. Plan view of distribution of surface temperatures in MHB for EMM model run at maximum flood. Vertical cross-sectional view of the plume from the outfall is shown in the insert.

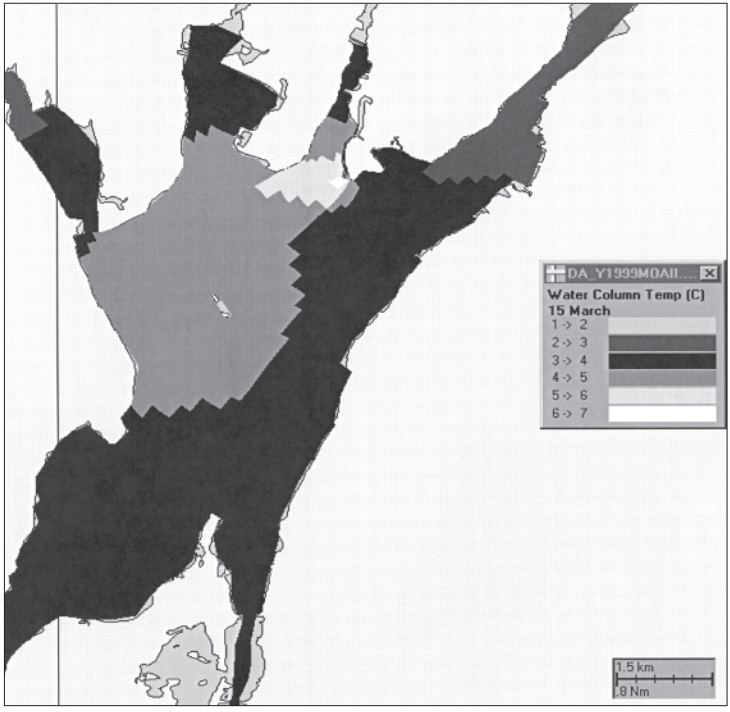

Figure 14. Plan view of daily mean water-column temperature for MOA II hydrothermal model run on March 15, 1999.

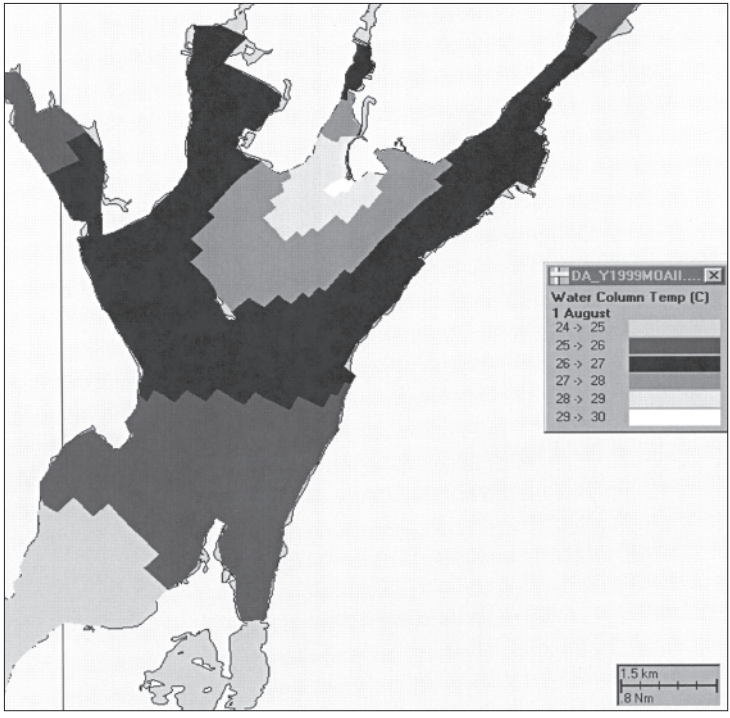

Figure 15. Plan view of daily mean water-column temperature for MOA II hydrothermal model run on August 1, 1999.

Figure 16. Plan view of daily mean water-column temperature for enhanced multimode hydrothermal model run on March 15, 1999.

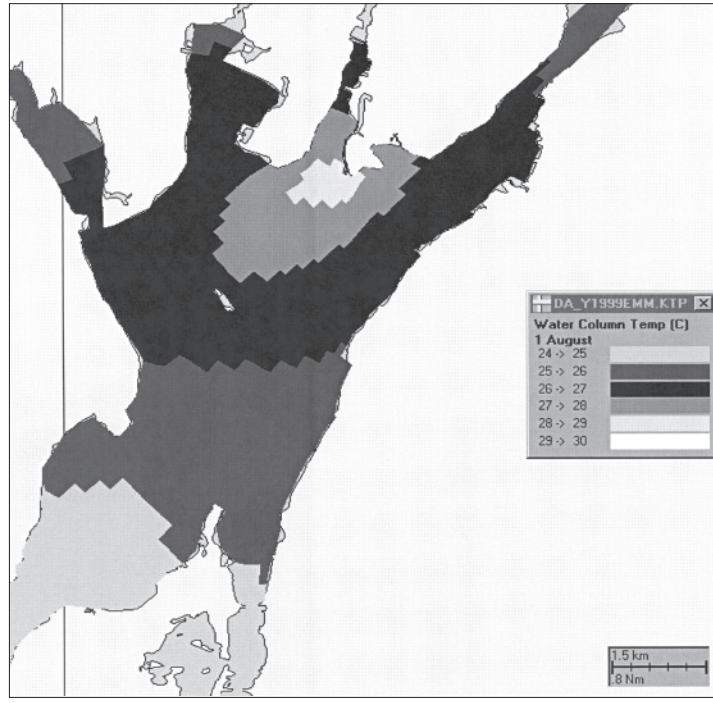

Figure 17. Plan view of daily mean water-column temperature for enhanced multimode hydrothermal model run on August 1, 1999.

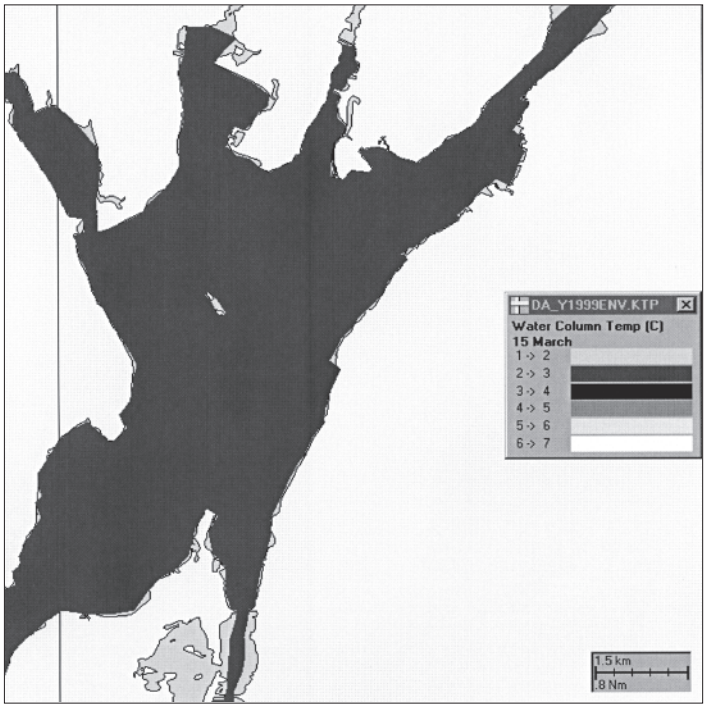

Figure 18. Plan view of daily mean water-column temperature for no-Plant hydrothermal model run on March 15, 1999.

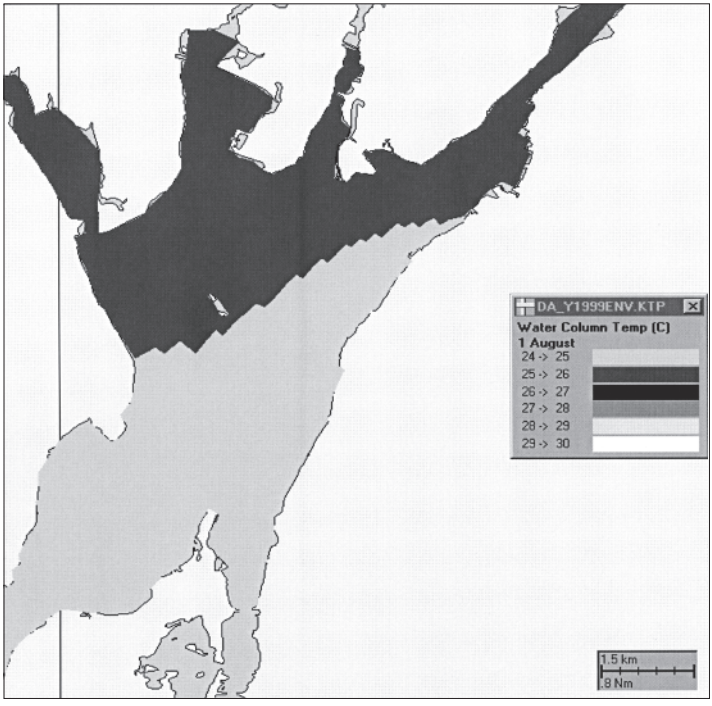

Figure 19. Plan view of daily mean water-column temperature for no-Plant hydrothermal model run on August 1, 1999.

As would be expected, the no-plant case results in slightly cooler temperatures for much of MHB. The temperature increases over ambient conditions were determined by subtracting the no-plant case from the MOAII and EMM cases. An average wind of 6 m s^{-1} blowing towards the south on March 15th generated a strong current in the southeast direction and caused the plume to spread in that direction. On August 1, the average wind of 3.6 m s^{-1} towards the east induced a much weaker current causing less spreading of the plume. Thus, the difference in orientation and extent of the plumes on March 15th and August 1st for all three forcing cases (Figs. 14–19) can be attributed to the difference in the wind on those days. March 15th and August 1st were chosen to represent, respectively, the spring and summer conditions for the seasonal variation of freshwater flow and heat flux.

Figures 20 and 21 show plan view of temperature differences for the EMM hydrothermal model run relative to the no-plant at maximum ebb and maximum flood, respectively. The effects of tide on the plume seen in Figures 20 and 21 is very similar to that exhibited in Figures 12 and 13. At maximum ebb, the thermal plume extends in the south-southwest direction (Fig. 20), since the ebb current moves in that direction. As the

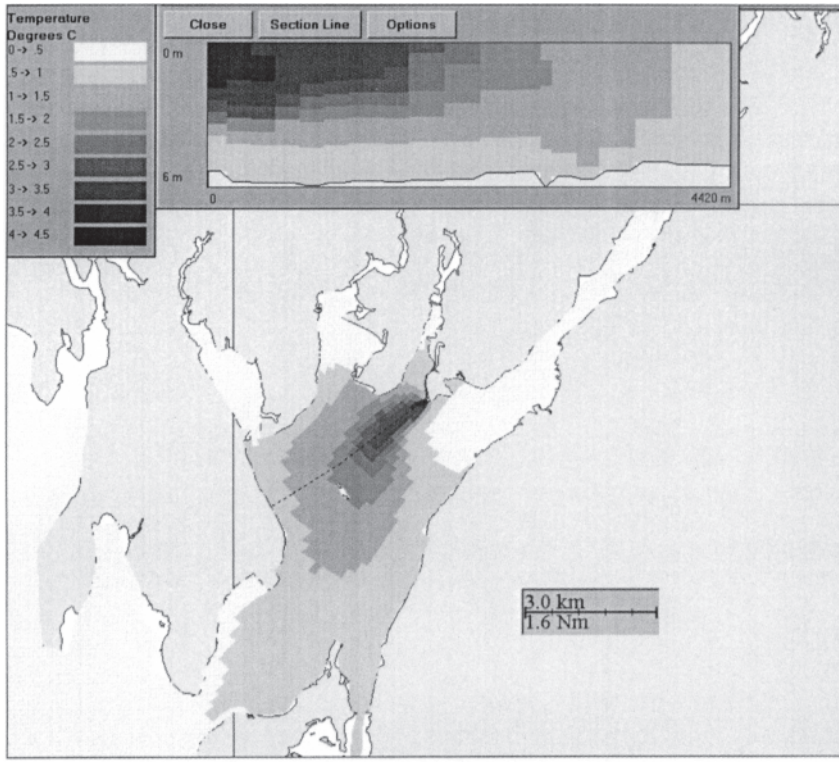

Figure 20. Plan view of surface temperature differences for the EMM hydrothermal model run relative to the no-plant run at maximum ebb. Vertical cross-sectional view from the outfall is seen in the insert.

tide turns, the plume generated during the previous ebb is moved north, while the plume generated during the flood moves towards the mouth of the Taunton River. At maximum flood (Fig. 21) the remnants of the ebb plume are seen to the west of the Station discharge, while the just-discharged flood plume is seen to the east.

Another comparison of the relative effects of the various scenarios is shown in Figure 22. Here, the cumulative percent of the volume of the Bay that is greater than a specific temperature is displayed against that temperature for the different Station loads. This analysis indicates how much of the Bay is subject to different temperature regimes. The analysis was based on the daily averaged temperatures over the simulated worst-case warm year (1999). The no-plant scenario shows the lowest volume at all temperatures and the MOAII scenario (current operating condition) typically shows the largest volume, with the EMM scenario (reduced heat operating condition) falling between the two, consistent with Station load. The difference in volume between the cases at a given temperature is small, however. For example, at 5 °C, the no-plant scenario shows 72% coverage compared to 82% coverage for the MOAII scenario. Similarly,

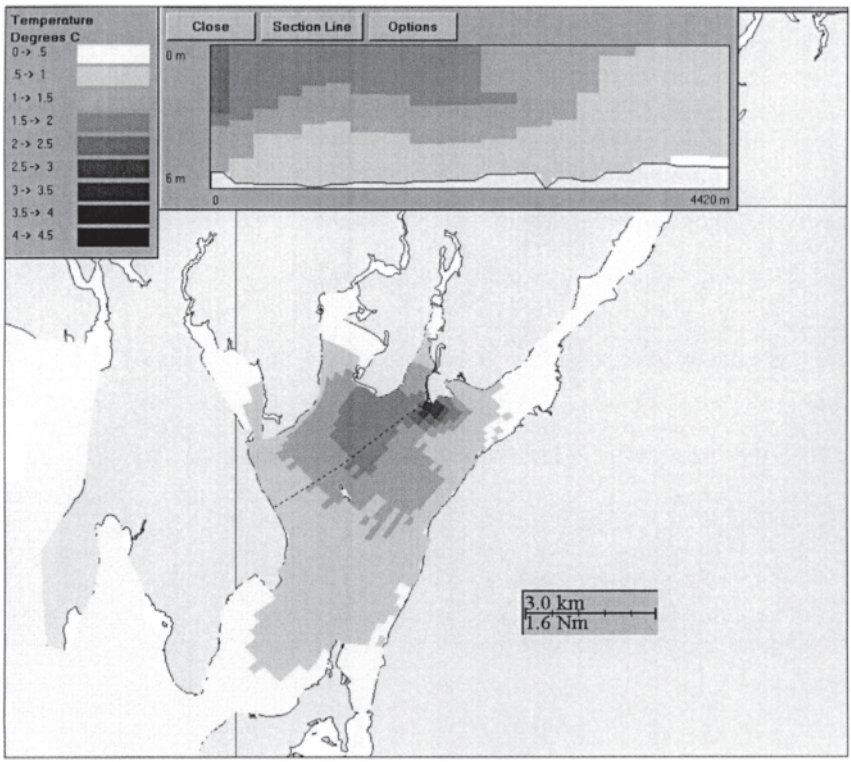

Figure 21. Plan view of surface temperature differences for the EMM hydrothermal model run relative to the no-plant run at maximum flood. Vertical cross-sectional view from the outfall is seen in the insert.

at 15 °C, the no-plant scenario shows 39% coverage compared to 43% coverage for MOAII, and at 25 °C, No-Plant gives 1% coverage and MOAII gives 5% .

The WQMAP model with a coarser grid (to keep run times reasonable) was also run for the four-decade period from 1960 to 1999, with environmental (no-plant) forcing to provide information on ambient (environmental background) conditions. The model results were averaged by day over the period and subsequently analyzed to reveal that 1999 was the second warmest year, which confirmed its selection as a reasonable worst-case warm year.

Presentation of the model results is found in a summary of hydrodynamic results (Swanson et al. 2001), the variance request (USGenNE 2001), and the Section 308 Information Request Response (ASA and LMS 2001).

Summary and Conclusions

A two-component hydrothermal assessment was conducted to understand the effects of the Brayton Point Station on MHB over different seasons and years. The first component, an extensive field data program, was designed and executed to provide physical data, with the short- and long-term temperature structure of the Bay being the primary focus. Very large data sets were acquired for use in characterizing the plume as it presently

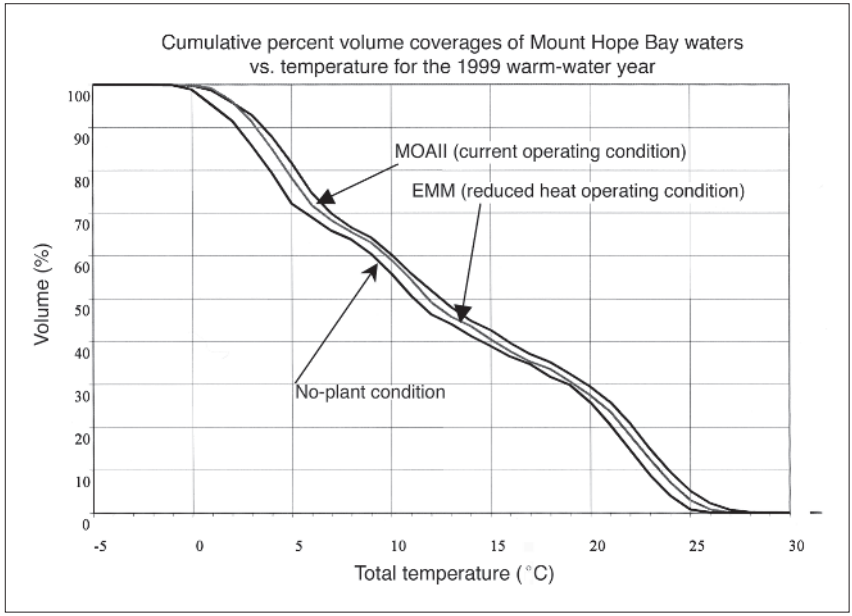

Figure 22. Volume coverage as a function of temperature over the 1999 yearly simulation for various Brayton Point Station heat loads: MOA II (current operating condition), EMM (reduced heat operating condition), and no-plant operating scenarios.

exists as well as for use in a hydrothermal model. The thermal plume from the Station is typically in the upper part of the water column and often confined at or near the surface and is principally located in the northern reaches of the Bay adjacent to the Station.

The second component was the application of a hydrothermal model that predicted the three-dimensional, time-varying distribution of temperature in MHB under the influence of both ambient conditions (i.e., without Brayton Point Station) and thermal loading from the Station. The model was successfully calibrated and verified to the data sets collected during the field programs and accepted for use as a tool to evaluate thermal effects by the Station Technical Advisory Committee.

The model was then used to examine a variety of Station operations, both historical and hypothetical, and their effect on the temperature of MHB during different seasons and years, particularly summer and winter periods of 1999, a warm year. It was found that the resulting temperature variations induced by the Station discharge are small relative to the natural thermal variations in the Bay. The Station has an incremental effect on the natural distribution of temperature.

A series of data products was developed for use in the subsequent biothermal assessment to determine the extent of biological impacts the Station may have on the communities that inhabit or use the Bay for various life cycles at various times during the year (O'Neill et al. 2005, USGenNE 2001). These products were designed to distill an immense amount of model-generated data to provide a rational analysis of temperature effects.

Literature Cited

Applied Science Associates, Inc. (ASA). 1996. Data report New England Power Company Brayton Point Station dissolved oxygen assessment field studies. Report to New England Power Co., Westborough, MA. December 1996.

Applied Science Associates, Inc., and Lawler, Matusky, and Skelly Engineers LLP (ASA and LMS). 2001. Supplemental hydrothermal and biothermal evaluation. Report to the US Environmental Protection Agency, Boston, MA, on behalf of Brayton Point Station.

Chen, C., H. Liu, and R.C. Beardsley. 2003. An unstructured, finite-volume, three-dimensional, primitive equation ocean model: Application to coastal ocean and estuaries. Journal of Atmospheric and Oceanic Technology 20:159–186.

Edinger, J.E., D.K. Brady, and J.C. Greyer. 1974. Heat exchange and transport in the environment, Report No. 14, Cooling Water Research Project (RP-49), Electrical Power Research Institute, Palo Alto, CA.

Fisher, J.A., and J.F. Mustard. 2004. High spatial resolution sea surface climatology from Landsat thermal infrared data. Remote Sensing of Environment 90:293–307.

Huang, W., and M.L. Spaulding. 1995a. Modeling of CSO-induced pollutant transport in Mount Hope Bay. Journal of Environmental Engineering 121(7):492–498.

Huang, W., and M.L. Spaulding. 1995b. A three-dimensional numerical model of estuarine circulation and water quality induced by surface discharges. Journal of Hydraulic Engineering 121(4):300–311.

Kim, H.-S., and J.C. Swanson, 2001. Modeling of double flood currents in the Sakonnet River. 7th Annual International Conference on Estuarine and Coastal Modeling (ECM 7), St. Pete Beach, FL. November 5–7, 2001.

McCutcheon, S.C., Z. Dongwei, and S. Bird. 1990. Model calibration, validation, and use. Chapter 5, *In* J.L. Martin, R.B. Ambrose and S.C. McCutcheon (Eds.). Technical Guidance Manual for Performing Waste Load Allocations, Book III: Estuaries. Part 2: Application of Estuarine Waste Load Allocation Models. Office of Water, USEPA, Washington, DC. March 1990.

Muin, M., and M.L. Spaulding. 1996. Two-dimensional boundary fitted circulation model in spherical coordinates. Journal of Hydraulic Engineering 122(9):512–521.

Muin, M., and M.L. Spaulding. 1997a. Three-dimensional boundary fitted circulation model. Journal of Hydraulic Engineering 123(1):2–12.

Muin, M., and M.L. Spaulding. 1997b. Application of three-dimensional boundary fitted circulation model to the Providence River. Journal of Hydraulic Engineering 123(1):13–20.

National Geophysical Data Center (NGDC). 1996. National Ocean Service, hydrographic survey data, Geophysical Data System (GEODAS) for hydrographic survey data. National Geophysical Data Center, NOAA, Boulder, CO.

O'Neill, R.J., T.L. Englert, and J.K. Ko, 2005. Effects of Brayton Point Station's thermal discharge on Mount Hope Bay winter flounder, Northeastern Naturalist 13(Special Issue 4): 71–94.

Ries, K.G. 1990. Estimating surface-water runoff to Narragansett Bay, Rhode Island and Massachusetts. Water Resources Investigations Report 89-4164. US Geological Survey, Denver, CO.

Rines, H. 1998. Mapping temperature distributions in Mount Hope Bay with respect to the Brayton Point Station outfall. Report to NEPCo. ASA, Narragansett, RI. April 1998.

Rines, H. 1999. Mapping temperature distributions in Mount Hope Bay, Fall 1998 deployment. Report to NEPCo. ASA, Narragansett, RI. September 1999.

Rines, H., and H. Schuttenberg. 1998. Data report New England Power Company, Brayton Point Station, Mount Hope Bay field studies for 1997. Report to NEPCo., Westborough, MA. ASA, Narragansett, RI. April 1998.

Spaulding, M.L. 1984. A vertically averaged circulation model using boundary fitted coordinates. Journal of Physical Oceanography 14:973–982.

Spaulding, M.L., D. Mendelsohn, and J.C. Swanson. 1999a. WQMAP: An integrated three-dimensional hydrodynamic and water quality model system for estuarine and coastal applications. Marine Technology Society Journal 33(3):38–54.

Spaulding, M.L., J.C. Swanson, and D. Mendelsohn. 1999b. Application of quantitative model–data calibration measures to assess model performance. Estuarine and Coastal Modeling 6 (ECM6), New Orleans, LA. November 3-5, 1999.

Swanson, J.C., M.L. Spaulding, J.P. Mathisen, and O.O. Jenssen. 1989. A three-dimensional, boundary-fitted coordinate hydrodynamic model, Part I: Development and testing. Deutsche Hydrographische Zeitschrift 42(1989):169–186.

Swanson, J.C., D. Mendelsohn, H. Rines, and H. Schuttenberg. 1998. Mount Hope Bay hydrodynamic model calibration and confirmation. Report to NEPCo, Westborough, MA. ASA, Narragansett, RI. May 1998.

Swanson, J.C., H. Rines, D. Mendelsohn, T. Isaji, and M. Ward. 1999. Mount Hope Bay winter 1999 field data and model confirmation. Report to PG&E National Energy Group, Somerset, MA. ASA, Narragansett, RI. October 1999.

Swanson, J.C., H.S. Kim, T. Isaji, and M. Ward. 2001. Summary of hydrodynamic model results for Brayton Point Station simulations. Report to PG&E National Energy Group, Somerset, MA. ASA, Narragansett, RI. January 2001.

United States Environmental Protection Agency–New England (USEPA-NE). 2002. Clean water act NPDES permitting determinations for thermal discharge and cooling water intake from Brayton Point Station in Somerset, MA. NPDES Permit No. MA 0003654, Boston, MA, 22 July 2002.

USGen New England, Inc. (USGenNE). 2001. Demonstration in support of NPDES Renewal NPDES Permit No. MA0003654. USGen New England, Brayton Point Station, Somerset, MA, December, 2001.